Jurnal Pena Sains Vol. 6, No. 1, April 2019
p-ISSN: 2407-2311
e-ISSN: 2527-7634

OXIDATION BEHAVIOR OF Zr-BASED AMORPHOUS ALLOYS AT 400˚- 450˚C IN AIR

Triwikantoro[1], Romdhoni Graha Pribadi[2], Fatimatul Munawaroh[3]

[1] Department of Physics, Faculty of Science, Institute Technology of Sepuluh Nopember Surabaya 60111 Indonesia
triwi@physics.its.ac.id

[2] Department of Physics, Faculty of Science, Institute Technology of Sepuluh Nopember Surabaya 60111 Indonesia
romdhoni_graha@yahoo.co.id

[3] Natural Science Education Study Program, Faculty of Education, University of Trunojoyo Madura Bangkalan, 69162, Indonesia
fatim@trunojoyo.ac.id

Accepted: February 23, 2019 ***Published: April 30, 2019***

DOI: http://doi.org/10.21107/jps.v6i1.5232

ABSTRACT

The study of oxidation behavior of amorphous alloys based on Zirconium with 2 variations in composition was carried out: $Zr_{64.5}Cu_{17}Ni_{11}Al_{7.5}$ and $Zr_{69.5}Cu_{12}Ni_{11}Al_{7.5}$ at temperatures of 400 - 450˚C in air. Amorphous Zr-based alloys were thermally characterized using Differential Scanning Calorimeter (DSC) to determine the crystallization temperature and glass transition temperature. The oxidation characterization was carried out using a Thermo gravimetric Analyzer (TGA) at temperatures of 400, 425, and 450˚C for 4 hours in air. The phase analysis of the oxidation product was identified using X-Ray Diffaction (XRD). Based on DSC data the crystallization temperature for $Zr_{64.5}Cu_{17}Ni_{11}Al_{7.5}$ and $Zr_{69.5}Cu_{12}Ni_{11}Al_{7.5}$ is 426 and 442˚C respectively. The oxidation kinetics of the two alloys follows parabolic law and the oxidation rate increases with the addition of temperature. Oxides formed during isothermal oxidation in the $Zr_{64.5}Cu_{17}Ni_{11}Al_{7.5}$ and $Zr_{69.5}Cu_{12}Ni_{11}Al_{7.5}$ alloys are t-ZrO_2 (tetragonal) as the dominant phase and ZrO_2 (monoclinic) and CuO as the minor phase. The intermetallic phase is also formed in samples, t-Zr_2Ni and Zr_2Cu.

Keywords: ***oxidation, amorphous alloy, oxide, intermetallic phase***

[1] Corresponding Author

Introduction

Research related to Zirconium-based metallic glass material has been carried out. Zirconium as a compound element is used as an reinforcement in steelmaking, porcelain, sports equipment such as golf and racket sticks, and many other applications (Appel, 2000; Mondal, Chatterjee, & Murty, 2007; Telford, 2004). Superior mechanical properties of Zirconium alloys such as high strength, large elasticity limits, good corrosion resistance, low appearance of neutron uptake, resistance to irradiation effects, and other mechanical properties make this material widely studied by researchers (Nikulina, Markelov, & Peregud, 1996; Shin, Jeong, Choi, & Inoue, 2007; W. Zhang, Jia, Zhang, & Inoue, 2007). However, in the high temperature the superior properties of Zirconium based metallic glass will be degraded namely amorphous structure stability and oxidation resistance (Köster & Jastrow, 2007; Neogy et al., 2004; Triwikantoro, Toma, Meuris, & Köster, 1999; Zander & Köster, 2004).

The oxidation resistance of an alloy can be seen from the character of the TGA curve, namely the addition or reduction of mass per unit area as a function of time. Zirconium-based amorphous alloy oxidation kinetics follow parabolic law and the oxidation rate increases with increasing temperature (Kai et al., 2009; Mondal et al., 2007; Triwikantoro & Munawaroh, 2008; Triwikantoro et al., 1999). Determination of heating temperature depends on the rate of heating used in the DTA-TG equipment to obtain the value of the glass transition temperature (T_g) and the crystallization temperature (T_x). The increase in T_g and T_x due to the increase in the heating rate is also accompanied by an increase in super cooled liquid areas which indicate that T_g and T_x for bulk amorphous alloys are an area of a certain range (Inoue, Zhang, Nishiyama, Ohba, & Masumoto, 1994). In isothermal oxidation for zirconium-based amorphous alloys above the crystallization temperature, it is found that the oxidation rate increases when the temperature is raised, whereas on Zirconium-based Nano crystal alloys the higher the temperature, the lower the oxide rate. The structure has a significant effect on the oxidation rate (Destyorini, Rudyardjo, & Triwikantoro, 2015; Kluge & John, 2015; Köster & Jastrow, 2007).

In this paper the results of the study of zirconium-based amorphous alloy oxidation behavior have been reported for more than 20 years. The study focused on the oxidation behavior above the crystallization temperature in the air to determine the oxidation resistance and the stability of the amorphous structure of the alloy. Identification of the phase of the oxide phase formed and the intermetallic phase is used as an indicator that the alloy has been oxidized and crystallized. The formation of the oxide phase indicates that the alloy is not resistant to oxidation, while the formation of crystals shows that the stability of the amorphous structure has been degraded.

Research Method

The amorphous Zr-based alloys with a variation of composition were arc-melted Zr, Cu, Ni and Al (> 99,9%) to produce of pre-alloy, then were fabricated by melt-spinning as described elsewhere in detail (Triwikantoro et al., 1999). These amorphous alloys have been stored on the plastic in a carton box for more than 20 years. The initial conditions of the samples were tested using Differential Scanning Calorimeter (Type DSC-60 Schimadzu) with heating rate 5˚/min and 10˚/min to know the crystallization

temperature, then the structure was investigated using XRD. Furthermore, based on thermal character data of DSC the samples were isothermally oxidized with various temperatures 400, 425 and 450˚C during 4 hours in air using TGA. Finally, the oxidized Zr-based amorphous alloys were characterized using XRD to reveal the formed phases after isothermal oxidation treatment.

Results and Discussion

Data from DSC observations are shown in Table 1. The T value (onset) in Table 1 shows the beginning of the transformation, while T_x is the crystallization temperature. The results of thermal characterization using DSC (*Differential Scanning Calorimeter*) showed that the value of the crystallization transition temperature depends on the heating rate and the alloy composition of the sample.

Table 1. Data of DSC testing with variation of heating rate

Sample	Heating rate (°C/min.)	T_{onset} (°C)	T_x (°C)
$Zr_{64.5}Cu_{17}Ni_{11}Al_{7.5}$	5	402.2	416.9
	10	418.0	426.2
$Zr_{69.5}Cu_{12}Ni_{11}Al_{7.5}$	5	423.0	433.6
	10	436.9	442.3

The highest crystallization temperature was found in the sample $Zr_{69.5}Cu_{12}Ni_{11}Al_{7.5}$ which was 442.3˚C with a heating rate of 10˚/min, while the lowest crystallization temperature was found in the sample $Zr_{64.5}Cu_{17}Ni_{11}Al_{7.5}$ which was 416.9˚C for a heating rate of 5˚C/min. The magnitude of the heating rate causes the crystallization temperature to shift in a larger direction (see Table 1.). In addition, the shift in temporal crystallization is also caused by the large composition of Zirconium elements. The greater the Zirconium composition, the greater the T_x. In addition, the Cu element also affects the formation of the amorphous phase into the crystalline phase. The addition of copper alloying elements results in an increase in the reconnaissance rate because Cu atoms have the ability to diffuse to form a more stable crystal structure (Triwikantoro & Fajarin, 2009). The heating rate also affects the crystallization temperature value. This is related to the super cooled liquid area that is formed. Increased T_g and T_x due to increased heating rates accompanied by increased super cooled liquid areas (Q. C. Zhang, Pang, Li, & Zhang, 2011).

The TGA test results from the alloys $Zr_{64.5}Cu_{17}Ni_{11}Al_{7.5}$ and $Zr_{69.5}Cu_{12}Ni_{11}Al_{7.5}$ are presented in Figures 1 and 2. The figure shows changes in mass as a function of time at temperatures of 400˚C, 425˚C, and 450˚C for 4 hours in air. An increase in mass occurs when isothermal oxidation is carried out. Zirconium has a Pilling-Bed worth ratio of 1.56, so the formed oxide is compacting not porous.

The formation of this oxide layer occurs because of the diffusion of oxygen ion ions through the compact oxide layer and the diffusion of metal ions towards the oxide/metal boundary plane, also diffusion of metal ion ions through the oxide layer and reacting at the oxide / gas face boundary. The reaction of oxygen ion ions and metal ion ions in these two face limits increases the thickness of the oxide layer (Birks & Meier, 1983).

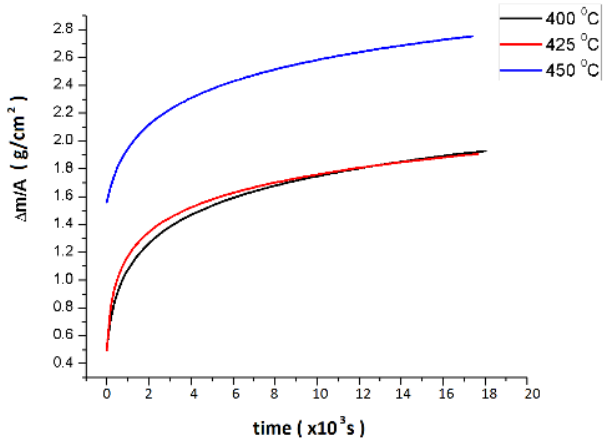

Figure 1. Kinetics of oxidation of the alloy $Zr_{64.5}Cu_{17}Ni_{11}Al_{7.5}$ at 400, 425 and 450˚C for 4 hours in air

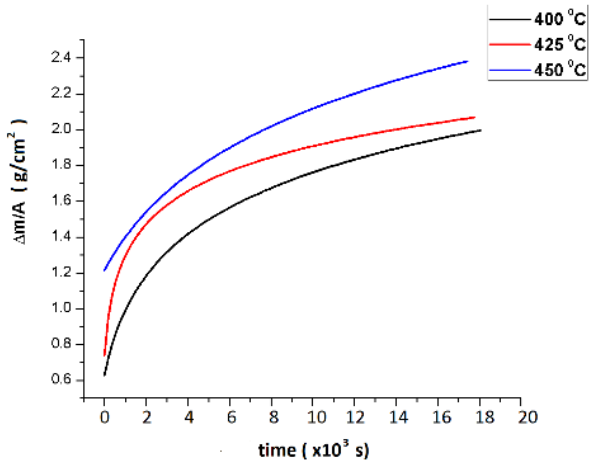

Figure 2. Oxidation kinetics of the alloy $Zr_{69.5}Cu_{12}Ni_{11}Al_{7.5}$ at 400, 425 and 450˚C for 4 hours in air

The oxidation kinetics of the $Zr_{64.5}Cu_{17}Ni_{11}Al_{7.5}$ and $Zr_{69.5}Cu_{12}Ni_{11}Al_{7.5}$ alloys follow parabolic functions and their kinetic constants can be determined by graphing the relationship of changes in mass per unit area (Δm/A) with time during isothermal oxidation. This law of parabolic oxidation kinetics is also in accordance with observations made by several researchers (Kai et al., 2009; Triwikantoro & Munawaroh, 2008; Triwikantoro et al., 1999) and also one stage parabolic and two stage parabolic kinetics (Cao, Zhang, & Shek, 2013; Chen, 2013; Hu, Cao, & Shek, 2014; M. Zhang, Yao, Wang, & Deng, 2014). The value of the oxidation rate constant (K_p) can be seen in Table 2.

Table 2. Value of the oxidation rate constant

Combining	K_p ($mg^2\ cm^{-4}\ s^{-1}$)		
	400˚C	425˚C	450˚C
$Zr_{64.5}Cu_{17}Ni_{11}Al_{7.5}$	1.3×10^{-4}	1.5×10^{-4}	2.3×10^{-4}
$Zr_{69.5}Cu_{12}Ni_{11}Al_{7.5}$	1.5×10^{-4}	1.7×10^{-4}	2.4×10^{-4}

The value of the oxidation rate is constant increases with increasing temperature. Increasing the temperature causes the thermal energy received by the Zirconium alloy to increase. This energy is used by alloys to react with oxygen from outside air. At high temperatures, the atmosphere is oxidative and has the potential for oxidation reactions with metal ions (Birks & Meier, 1983).

The phase formation after the isothermal oxidation treatment with TGA can be identified using XRD. Figures 3 and 4 shows that the diffraction pattern of the alloy after oxidation, which can indicate the oxidation product. In Figures 3 and 4 the oxide product is identified, namely t-ZrO_2 (tetragonal) as the dominant phase and t-CuO (tetragonal) and m-ZrO_2 (monoclinic) as the minor phase. In addition, the intermetallic phase t-Zr_2Ni (tetragonal) and t-Zr_2Cu (tetragonal) are also identified. The phase t-ZrO_2 (tetragonal) is the dominant phase. This is because Zirconium has a low oxidation potential with oxygen, so it is easy to react with oxygen to form oxides. The t-Zirconia phase evaporates the metastable phase. The increase in temperature and the length of the isothermal oxidation phase m-ZrO_2 will be formed. In the Zr-O Phase diagram system there are three types of changes, Monoclinic ZrO_2 is formed under temperatures of 1000-1200C, tetragonal ZrO_2 is stable at higher temperatures, and cubic ZrO_2 is stable above 1500 ° C. The formation of t-ZrO_2 and m-ZrO_2 oxides after isothermal oxidation around T_g and T_x was also observed by several researchers (Chen, 2013; Kai et al., 2009; Kim, Jeong, & Lee, 2008; Köster & Jastrow, 2007; Lim et al., 2014; Triwikantoro et al., 1999), as well as the minor oxide Al_2O_3 phase (Kai et al., 2009).

In some temperature conditions it is seen that the amorphous phase has slowly begun to disappear with the appearance of the ZrO_2 phase in each variation of heating. An increase in temperature will cause an increase in thermal energy received by amorphous material. Increasing thermal energy causes the nucleus to grow by attracting other atoms from the nucleus that have not yet had time to grow to fill the empty space in the lattice that will be formed. With increasing thermal energy received by amorphous material, the crystal growth continues until the final transformation is obtained from amorphous to crystalline.

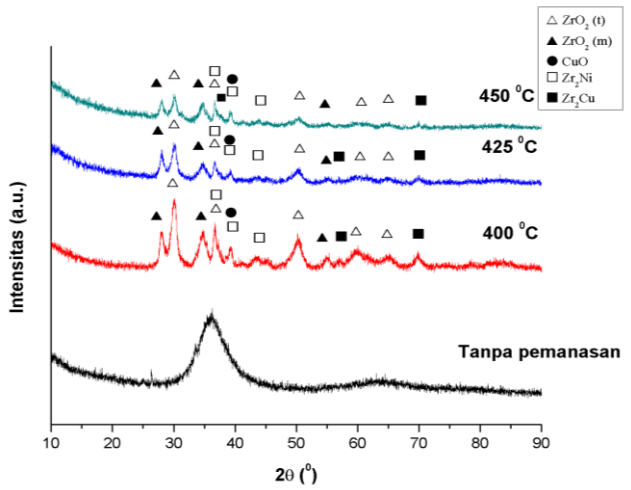

Figure 3. Diffraction Patterns of X-rays of $Zr_{64.5}Cu_{17}Ni_{11}Al_{7.5}$ alloy after oxidation variation temperatures

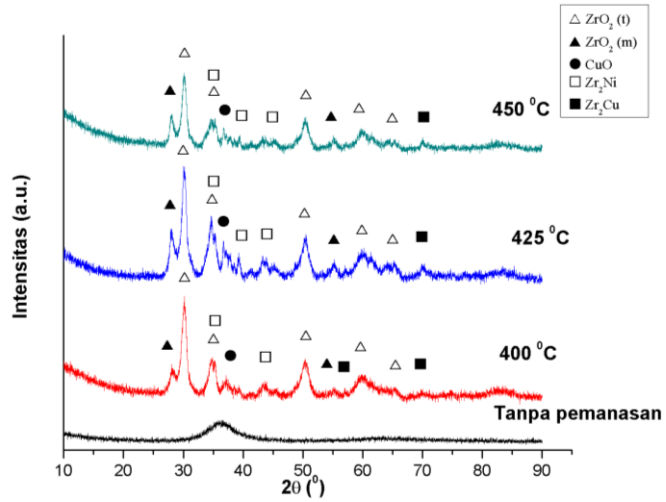

Figure 4. Diffraction Patterns of X-rays of $Zr_{69.5}Cu_{12}Ni_{11}Al_{7.5}$ alloy after oxidation with varying temperatures.

The intermetallic phase formed shows that at temperatures between 400-450^{o}C Zirconium alloy samples are crystallized. This reinforces the DSC curve data that the crystallization temperature of Zirconium-based amorphous alloys occurs at temperatures between 400-450˚C, namely 426^{o}C for $Zr_{64.5}Cu_{17}Ni_{11}Al_{7.5}$ and 442˚C for $Zr_{69.5}Cu_{12}Ni_{11}Al_{7.5}$.

The formation of CuO oxide products as a minor phase is associated with a small composition of Cu alloys. The CuO phase formation as a minor phase is inseparable from the chemical affinity that Cu has lower than that of Zr in metallic glass alloys. Cu and electron ions move outward and oxygen ions move inward. This reaction occurs in the oxide layer. As long as Cu oxidation diffuses predominantly outward, oxygen into (Wang et al., 2012).

Conclusion

Based on the results of this study it can be concluded that the heating temperature has a significant effect on isothermal oxidation on Zirconium-based amorphous alloys. Zirconium-based amorphous alloy oxidation kinetics follows parabolic law with the oxidation rate increasing with increasing temperature. The phases formed after isothermal oxidations are t-$Zr0_2$ as the dominant phase while m-ZrO_2 (monoclinic) and t-CuO as the minor phase and the intermetallic phase t-Zr_2Ni and t-Zr_2Cu are formed.

Acknowledgment

The author would like to thank the BCI Research Group, Faculty of Chemical Engineering, and TU Dortmund, Germany for preparation of Zr-based amorphous alloys.

References

Appel, H. (2000). Physikalishe Aspekte des Golfspiels. *Physikalische Blatter*, **56** pp. 25 - 31.

Birks, N., & Meier, G. H. (1983). Introduction of to High Temperature Oxidations of Metals. London: Edward Arnold.

Cao, W. H., Zhang, J. L., & Shek, C. H.

(2013). The oxidation behavior of $Cu_{42}Zr_{42}Al_{8}Ag_{8}$ bulk metallic glasses. *Journal of Materials Science*, *48*(3), 1141–1146. https://doi.org/10.1007/s10853-012-6851-y

Chen, X. (2013). Structure and hardness evolution of the scale of a Zr-based metallic glass during oxidation. *Journal of Non-Crystalline Solids*, *362*(1), 140–146. https://doi.org/10.1016/j.jnoncrysol.2012.11.018

Destyorini, F., Rudyardjo, D. I., & Triwikantoro, T. (2015). Pengaruh Elemen Pemadu Terhadap Ketahanan Korosi Paduan Amorf Berbasis Zirkonium, *18*(1), 2015.

Hu, Y., Cao, W., & Shek, C. (2014). The corrosion and oxidation behavior of Zr-based metallic glasses. *Journal of Materials Research*, *29*(11), 1248–1255. https://doi.org/10.1557/jmr.2014.107

Inoue, A., Zhang, T., Nishiyama, N., Ohba, K., & Masumoto, T. (1994). Extremely wide supercooled liquid region and large glass-forming ability in $Zr_{65-x}Al_{7.5}Cu_{17.5}Ni_{10}Be_{x}$ amorphous alloys. *Materials Science and Engineering: A*, *179*, 210–214.

Kai, W., Chen, Y. R., Ho, T. H., Hsieh, H. H., Qiao, D. C., Jiang, F., Liaw, P. K. (2009). Air oxidation of a $Zr_{58}Cu_{22}Al_{12}Fe_{8}$ bulk metallic glass at 350-550 °C. *Journal of Alloys and Compounds*, *483*(1–2), 519–525. https://doi.org/10.1016/j.jallcom.2008.10.133

Kim, C. W., Jeong, H. G., & Lee, D. B. (2008). Oxidation of $Zr_{65}Al_{10}Ni_{10}Cu_{15}$ bulk metallic glass. *Materials Letters*, *62*(4–5),584–586. https://doi.org/10.1016/j.matlet.2007.06.010

Kluge, T., & John, C. M. (2015). Technical Note : A simple method for vaterite precipitation for isotopic studies : implications for bulk and clumped isotope analysis, 3289–3299. https://doi.org/10.5194/bg-12-3289-2015

Köster, U., & Jastrow, L. (2007). Oxidation of Zr-based metallic glasses and nanocrystalline alloys. *Materials Science and Engineering A*, *448–451*, 57–62. https://doi.org/10.1016/j.msea.2006.02.316

Lim, K. R., Park, J. M., Park, S. H., Na, M. Y., Kim, K. C., Kim, W. T., & Kim, D. H. (2014). Oxidation induced amorphous stabilization of the subsurface region in Zr-Cu metallic glass. *Applied Physics Letters*, *104*(3). https://doi.org/10.1063/1.4862025

Mondal, K., Chatterjee, U. K., & Murty, B. S. (2007). Oxidation behavior of multicomponent Zr-based amorphous alloys. *Journal of Alloys and Compounds*, *433*(1–2), 162–170. https://doi.org/10.1016/j.jallcom.2006.06.061

Neogy, S., Mukherjee, A., Ashwini, B., Srivastava, D., Savalia, R. T., Dey, G. K., De, P. K. (2004). Zirconium Based Bulk Metallic Glass/Tungsten Fibre Composite-Fabrication and Characterization". *International Symposium of Reseacrh Student on Materials Science and Engineering, Department of Metallurgical and Materials Engineering, Indian Institute of Technology Madras, Chennai*, 1–12. Retrieved from http://onlinelibrary.wiley.com/doi/10.1002/cbdv.200490137/abstract

Nikulina, A. V., Markelov, V. A., & Peregud, M. M. (1996). ”Zirconium Alloy E635 as a Material for Fuel Rod Cladding and Other Components of WWER and RBMK Cores”. Zirconium in Nuclear

Industry , Eleventh International Symposium. *Zirconium in Nuclear Industry , Eleventh International Symposium.*

Shin, H. S., Jeong, Y. J., Choi, H. Y., & Inoue, A. (2007). Influence of crystallization on the deformation behavior of $Zr_{55}Al_{10}Ni_5Cu_{30}$ bulk metallic glass in the supercooled liquid region. *Materials Science and Engineering A*, *448–451*, 243–247. https://doi.org/10.1016/j.msea.2006.02.290

Telford, M. (2004). The case for Bulk Metallic Glass. *Materials Today*, (March), 36–43.

Triwikantoro, T., & Fajarin, R. (2009). Pengaruh elemen pemadu pada kestabilan struktur paduan amorf berbasis zirkonium, 1–5.

Triwikantoro, T., & Munawaroh, F. (2008). Perilaku Oksidasi Paduan Gelas Metalik Zr-Cu-Ni-Al Pada 440-480^o C di Udara. *Prosiding Seminar Material Metalurgi 2008*, 271–275.

Triwikantoro, Toma, D., Meuris, M., & Köster, U. (1999). Oxidation of Zr-based metallic glasses in air. *Journal of Non-Crystalline Solids*, *250–252 (I*, 719–723. https://doi.org/10.1016/S0022-3093(99)00167-2

Wang, B., Huang, D. Y., Prud'Homme, N., Chen, Z., Jomard, F., Zhang, T., & Ji, V. (2012). Diffusion mechanism of Zr-based metallic glass during oxidation under dry air. *Intermetallics*, *28*, 102–107. https://doi.org/10.1016/j.intermet.2012.04.003

Zander, D., & Köster, U. (2004). Corrosion of amorphous and nanocrystalline Zr-based alloys. *Materials Science and Engineering A*, *375–377*(1–2 SPEC. ISS.), 53–59. https://doi.org/10.1016/j.msea.2003.10.230

Zhang, M., Yao, D., Wang, X., & Deng, L. (2014). Air oxidation of a $Zr_{55}Cu_{30}Al_{10}Ni_5$ bulk metallic glass at its super cooled liquid state. *Corrosion Science*, *82*, 410–419. https://doi.org/10.1016/j.corsci.2014.02.007

Zhang, Q. C., Pang, S. J., Li, Y., & Zhang, T. (2011). Correlation between supercooled liquid region and crystallization behavior with alloy composition of La-Al-Cu metallic glasses. *Science China: Physics, Mechanics and Astronomy*, *54*(9), 1608–1611. https://doi.org/10.1007/s11433-011-4434-6

Zhang, W., Jia, F., Zhang, Q., & Inoue, A. (2007). Effects of additional Ag on the thermal stability and glass-forming ability of Cu-Zr binary glassy alloys. *Materials Science and Engineering A*, *459*(1–2), 330–336. https://doi.org/10.1016/j.msea.2007.02.001